

## Peptide and glycopeptide dendrimer apple trees as enzyme models and for biomedical applications

Jean-Louis Reymond\* and Tamis Darbre

Received 18th November 2011, Accepted 19th December 2011

DOI: 10.1039/c2ob06938e

Solid phase peptide synthesis (SPPS) provides peptides with a dendritic topology when diamino acids are introduced in the sequences. Peptide dendrimers with one to three amino acids between branches can be prepared with up to 38 amino acids (MW ~ 5,000 Da). Larger peptide dendrimers (MW ~ 30,000) were obtained by a multivalent chloroacetyl cysteine (CIAC) ligation. Structural studies of peptide dendrimers by CD, FT-IR, NMR and molecular dynamics reveal molten globule states containing up to 50% of  $\alpha$ -helix. Esterase and aldolase peptide dendrimers displaying dendritic effects and enzyme kinetics ( $k_{\text{cat}}/k_{\text{uncat}} \sim 10^5$ ) were designed or discovered by screening large combinatorial libraries. Strong ligands for *Pseudomonas aeruginosa* lectins LecA and LecB able to inhibit biofilm formation were obtained with glycopeptide dendrimers. Efficient ligands for cobalamin, cytotoxic colchicine conjugates and antimicrobial peptide dendrimers were also developed showing the versatility of dendritic peptides. Complementing the multivalency, the amino acid composition of the dendrimers strongly influenced the catalytic or biological activity obtained demonstrating the importance of the “apple tree” configuration for protein-like function in peptide dendrimers.

### Introduction

Organic small molecules consist of sets of atoms connected through covalent bonds in various topologies, resulting in billions of possibilities.<sup>1</sup> At a higher level macromolecules result from the assembly of various monomers, which are themselves small organic molecules, to form oligomers and polymers. Among the possible topologies of such macromolecules, dendrimers form a family on their own consisting of regular molecular trees assembled from smaller dendrons as monomeric building blocks.<sup>2</sup> From the early days dendrimers were pictured as simplified mimics for proteins, in particular enzymes, due to a roughly globular shape enforced by the ramified topology rather than by folding.<sup>3</sup> However, while proteins consist of diverse amino acids throughout their structure, research focused on dendrimers based almost exclusively on an “ornamental tree” configuration in which functional molecules are present only either at the core or at the branch ends (Fig. 1A). The same principle was used for dendrimers assembled from amino acids, called peptide dendrimers, which consisted of a poly-lysine tree appended with multiple copies of linear peptides. These dendrimers were prepared for the purpose of increasing the biological activity of linear peptides by multivalent display, in particular antigenicity and antimicrobial activity.<sup>4</sup>

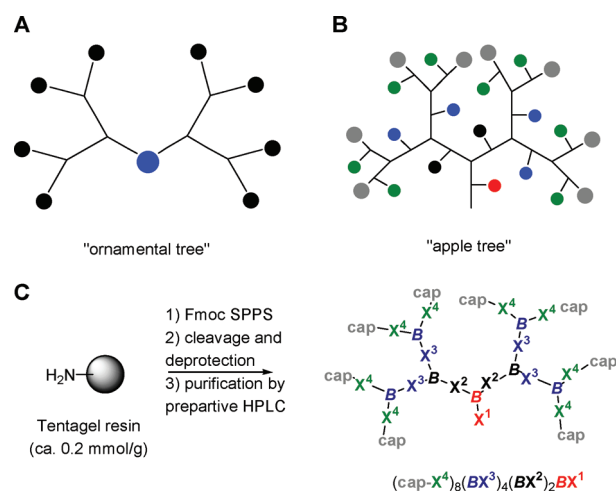


**Fig. 1** A. “Ornamental tree” configuration typical for dendrimers such as PPI (poly(propyleneimine), PAMAM (poly(amidoamine)), Fréchet’s dendrimers and poly-lysine trees. B. “Apple tree” configuration typical for the peptide dendrimers discussed here. C. Solid-phase peptide synthesis (SPPS) of peptide dendrimers. Standard Fmoc-protected amino acids are used for positions X, bis-Fmoc diamino acids (lysine, diamino-propanoic acid) are used at branching point positions (B). The branches may be extended to more than one amino acid (di-, tri- and tetra-peptide branches were also used). The capping group (cap) may be acetyl, a glycosyl group, or can be omitted. The amino acid sequence notation used in Table 1 is illustrated below the structure.

Department of Chemistry and Biochemistry, University of Berne/  
Freiestrasse 3, 3012 Berne, Switzerland. E-mail: jean-louis.reymond@  
ioc.unibe.ch; Fax: +41 31 631 8057; Tel: +41 31 631 4325

In 2003 our group reported a different type of peptide dendrimer in which the functional groups, presented as amino acid side chains, were distributed throughout the branches, a design corresponding to an “apple tree” configuration (Fig. 1B).<sup>5</sup> The synthesis capitalized on readily available amino acid building blocks and their assembly by solid-phase peptide synthesis (SPPS, Fig. 1C).<sup>6</sup> SPPS proved suitable for dendrimers up to G3 with eight N-termini and up to 38 amino acids (MW 4,700 Da), containing one to four amino acids per branch and various diamino acids as branching units. The branches of these dendrimers contained identical amino acids at equivalent positions when grown simultaneously in the divergent synthesis process by SPPS. The use of orthogonal protection schemes and the formation of asymmetrical disulfide-bridged dimers gave access to peptide dendrimers with up to four different types of branches.<sup>7</sup>

Our group has synthesized and purified over 400 different peptide and glycopeptide dendrimers in the course of the following studies: a) the optimization of combinatorial synthesis, decoding and screening protocols for peptide dendrimers and their use in structure–activity relationship studies of multivalent esterase and aldolase peptide dendrimers; b) the development of the multivalent chloroacetyl to cysteine (ClAc) ligation to prepare G4, G5 and G6 peptide dendrimers; c) structural studies by CD, FT-IR, NMR and molecular dynamics with the example of esterase peptide dendrimers with a single catalytic site at the core and of designed  $\alpha$ -helical peptide dendrimers; d) metallo-peptide dendrimers, including cobalamin ligands and bipyridine containing peptide dendrimers; e) the synthesis of glycopeptide dendrimers as drug delivery agents and as *Pseudomonas aeruginosa* biofilm inhibitors; f) membrane disrupting antimicrobial peptide dendrimers. The present review discusses key aspects of the structure–activity relationships in peptide dendrimers, which were uncovered by screening of peptide dendrimer combinatorial libraries as well as through systematic analoging. These studies were made possible by the reliability of SPPS for peptide dendrimers.

## Enzyme models

### Esterase peptide dendrimers as enzyme models

The ability of peptide dendrimers to perform catalysis in an aqueous environment was investigated first as a test for a typical protein function.<sup>8</sup> Combinatorial libraries of peptide dendrimers were prepared incorporating the catalytic triad amino acids aspartate, histidine and serine, and tested for activity using fluorogenic enzyme substrates.<sup>9,10</sup> These experiments showed that a strong positive dendritic effect occurred for the hydrolysis of fluorogenic 8-acyloxyppyrene-1,3,6-trisulfonates **1a–c** at the pH optimum of 5.5 under catalysis by peptide dendrimer **A3** (Fig. 2). The apparent rate accelerations in this system were as high as  $k_{\text{cat}}/k_{\text{uncat}} = 90\,000$  in the best dendrimer **A3C** with the butyryl ester **1b** as substrate (Table 1). This rate enhancement corresponds to an apparent reactivity increase of approximately 18 000 per catalytic site, an activity comparable to the best enzyme models for this type of reaction.<sup>11</sup> The effect was caused by: a) increased hydrophobic binding of the acyl group as evidenced by lower  $K_M$  values for higher generation dendrimers and for ester substrates with longer acyl chains; b) cooperative

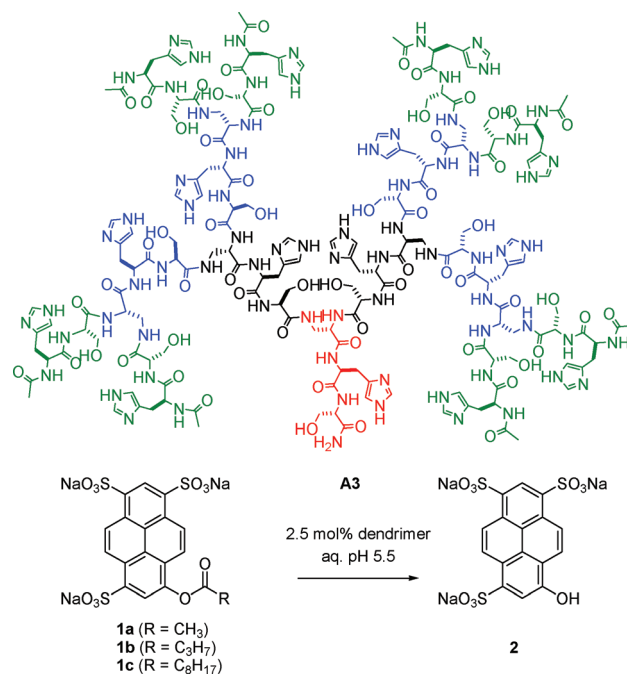


**Fig. 2** The multivalent esterase dendrimer **A3** catalyzes the hydrolysis of 8-acyloxyppyrene-1,3,6-trisulfonates **1a–c**.

effects between histidine side chains acting both as catalytic groups in free base form (general base or nucleophile) and for electrostatic substrate binding in the protonated form. The cooperativity was caused in part by a lowering of the histidine  $pK_a$  value within the multivalent dendrimer.

### Combinatorial studies of dendritic and linear peptide esterase and aldolase enzyme models

SPPS was readily adapted to the split-and-mix protocol to obtain “one-bead-one-compound” peptide dendrimer combinatorial libraries (Fig. 3a).<sup>12</sup> We initially performed “on-bead” assays with fluorogenic substrates to identify polymer beads carrying active dendrimers (Fig. 3b).<sup>9</sup> However in several cases we encountered poor reproducibility between the on-bead screening results and the activity of the re-synthesized, purified peptide dendrimers in solution, which we attribute to the very high concentration of peptide dendrimer on the beads. We therefore established an alternative “off-bead” assay using combinatorial libraries prepared on a photolabile resin.<sup>13</sup> In this assay the beads were photolysed without solvent to release the product, and spread onto a silica gel plate impregnated with a fluorogenic substrate solution. The peptide dendrimers diffused from the bead into the silica gel and a fluorescent halo was formed around beads carrying an active peptide dendrimer (Fig. 3c).

The “off-bead” assay was used for a structure–activity relationship study of the single-site esterase dendrimer **RG3** (AcYT)<sub>8</sub>(BWG)<sub>4</sub>(BRS)<sub>2</sub>BHS, which had been initially discovered using the on-bead assay.<sup>14</sup> Screening of the same 65 536-membered combinatorial dendrimer library used to discover **RG3** was performed using the “off-bead” assay with fluorogenic substrates **1b** and the corresponding (*R*)- or (*S*)-3-phenyl-butyrate. While no significant enantioselectivities were revealed, the off-bead assay confirmed that productive catalysis required

**Table 1** Examples of catalytic and bioactive peptides and peptide dendrimers

Name <sup>a</sup>	Sequence <sup>b</sup>	No. AA	MW	Property studied	Ref.
<b>A3</b>	(Ac-HS) <sub>8</sub> (BHS) <sub>4</sub> (BHS) <sub>2</sub> BHS	37	4317	catalyzes hydrolysis of <b>1a-c</b>	11a
<b>A3B</b>	(Ac-HβA) <sub>8</sub> (BHβA) <sub>4</sub> (BHβA) <sub>2</sub> BHβA	37	4077	catalyzes hydrolysis of <b>1a-c</b>	11b
<b>A3C</b>	(Ac-HT) <sub>8</sub> (BHT) <sub>4</sub> (BHT) <sub>2</sub> BHT	37	4525	catalyzes hydrolysis of <b>1a-c</b>	11b
<b>RG3</b>	(Ac-YT) <sub>8</sub> (BWG) <sub>4</sub> (BRS) <sub>2</sub> BHS	37	4752	catalyzes hydrolysis of <b>1a-c</b>	14
<b>HG3</b>	(Ac-IP) <sub>8</sub> (BIT) <sub>4</sub> (BHA) <sub>2</sub> BHL	37	4160	catalyzes hydrolysis of <b>1a-c</b>	14
<b>D3</b>	(Ac-ET) <sub>8</sub> (BIG) <sub>4</sub> (BHA) <sub>2</sub> BHL	37	4145	inactive analogs of <b>HG3</b>	13
<b>P65</b>	(Ac-YG) <sub>8</sub> (BYS) <sub>4</sub> (BKK) <sub>2</sub> BTH	37	4470	catalyzes hydrolysis of <b>1a-c</b>	16
<b>His7</b>	Ac-HHHHHHH	7	1020	catalyzes hydrolysis of <b>1a-c</b>	16
<b>L2D1</b>	(PK) <sub>8</sub> (BPK) <sub>4</sub> (BYL) <sub>2</sub> BIG	37	4046	catalyzes aldol reactions	20
<b>P5</b>	PFYLFhPVD	8	1011	catalyzes aldol reactions	22
<b>AcH3</b>	(Ac-H) <sub>8</sub> (KL) <sub>4</sub> (KV) <sub>2</sub> KK	22	3127	catalyzes hydrolysis of <b>9</b>	25
<b>H8</b>	(H) <sub>8</sub> (KβA) <sub>4</sub> (KT) <sub>2</sub> KaP	22	2609	catalyzes hydrolysis of <b>1a</b>	25
<b>G5P5</b>	(PS) <sub>32</sub> (BPS) <sub>16</sub> (PSCxHS) <sub>8</sub> (BHS) <sub>4</sub> (BHS) <sub>2</sub> BHS	181	17645	esterase and aldolase model	27
<b>G6P1</b>	(PS) <sub>64</sub> (BPS) <sub>32</sub> (BPS) <sub>16</sub> (BPSCxPS) <sub>8</sub> (BPS) <sub>4</sub> (BPS) <sub>2</sub> BPS	341	31588	catalyzes aldol reactions	27
<b>RG3H</b>	(Ac-YT) <sub>8</sub> (BWG) <sub>4</sub> (BHS) <sub>2</sub> BHS	37	4714	catalyzes hydrolysis of <b>1b</b>	34
<b>αD3</b>	(Ac-AMEA) <sub>4</sub> (KKLME) <sub>2</sub> KMKLA	31	3627	contains 50% α-helix	35
<b>B1</b>	(Ac-ES) <sub>8</sub> (BEA) <sub>4</sub> (KAmbY) <sub>2</sub> BCD	37	4379	binds to cobalamin	36
<b>B1K</b>	(Ac-KS) <sub>8</sub> (BKA) <sub>4</sub> (KAmbY) <sub>2</sub> BCL	37	4365	no binding to cobalamin	36
<b>N3</b>	(Ac-QS) <sub>8</sub> (BQA) <sub>4</sub> (KAmbY) <sub>2</sub> BCD	37	4283	binds to cobalamin	38
<b>E1</b>	(Ac-ET) <sub>4</sub> (BEV) <sub>2</sub> BBpyβAD	18	2203	binds to Fe(II)	39
<b>E3</b>	(Ac-RK) <sub>4</sub> (BFK) <sub>2</sub> BBpyβAY	18	2561	no binding to Fe(II)	39
<b>20</b>	(Glc-β-ON=Ac) <sub>8</sub> (BL) <sub>4</sub> (BD) <sub>2</sub> BC(SCol)H	22	3819	cytotoxic to cancer cells	43
<b>J1C</b>	(GalB-GRHA) <sub>2</sub> BTRHDC(Col)	14	2457	cytotoxic to cancer cells	44
<b>J1F</b>	(GalB-GRHA) <sub>2</sub> BTRHDC(Fluo)	14	2446	labels cancer cells	44
<b>FD2</b>	(cFuc-KPL) <sub>4</sub> (KFKI) <sub>2</sub> KHI	23	3536	biofilm inhibitor	50
<b>2G3</b>	(cFuc-KP) <sub>8</sub> (KLF) <sub>4</sub> (KKI) <sub>2</sub> KHI	37	5994	optimized ligand for LecB	51
<b>αFD2</b>	(cFuc-kpl) <sub>4</sub> (kfl) <sub>2</sub> khl	23	3536	biofilm inhibitor	52
<b>GalAG2</b>	(GalA-KPL) <sub>4</sub> (KFKI) <sub>2</sub> KHI	23	3909	biofilm inhibitor	53
<b>GalBG2</b>	(GalB-KPL) <sub>4</sub> (KFKI) <sub>2</sub> KHI	23	3783	biofilm inhibitor	53
<b>H1</b>	L <sub>8</sub> (KL) <sub>4</sub> (KF) <sub>2</sub> KK	22	2694	antimicrobial	58
<b>bH1</b>	L <sub>8</sub> (BL) <sub>4</sub> (BF) <sub>2</sub> BK	22	2401	antimicrobial	58
<b>D12</b>	(Ac-SA) <sub>8</sub> (BAR) <sub>4</sub> (BAD) <sub>2</sub> BFAK(Fluo)	38	4236	proteolysed by trypsin	59
<b>D18B</b>	(Ac-E) <sub>8</sub> (BF) <sub>4</sub> (BR) <sub>2</sub> BL	22	3003	protease resistant	59

<sup>a</sup> Compound number as used in the original publication; <sup>b</sup> Dendritic sequence notation with C-terminus at right using standard one-letter codes for amino acids, see figures for complete structural formulae. C-termini are carboxamide except for **H8** as acid, Ac = acetyl, B = branching 2,3-diaminopropionic acid, K = branching lysine, hP = hydroxyproline, βA = β-alanine, aP = (2S,4S)-4-aminoproline, x = thioether link between the side-chain cysteine thiol and the N-terminus of the next amino acid as S-CH<sub>2</sub>-CO, Amb = 4-aminomethyl benzoic acid, Bpy = 5'-Amino-2,2'-bipyridine-5-carboxylic acid, -ON=Ac = -O-N=CH-CO-, C(Col) = cysteine thioether formed by reaction with 7-chloroacetamido-colchicine, C(Fluo) = cysteine thioether formed by reaction with 4-iodoacetyl-fluorescein, GalB = β-galactosyl-3-thiopropionyl, cFuc = α-fucosyl-methylcarbonyl, GalA = 4 (β-galactosyloxy)benzoyl, K(Fluo) = 5/6-carboxyfluorescein linked by amide bond to the ε-amino group of lysine.

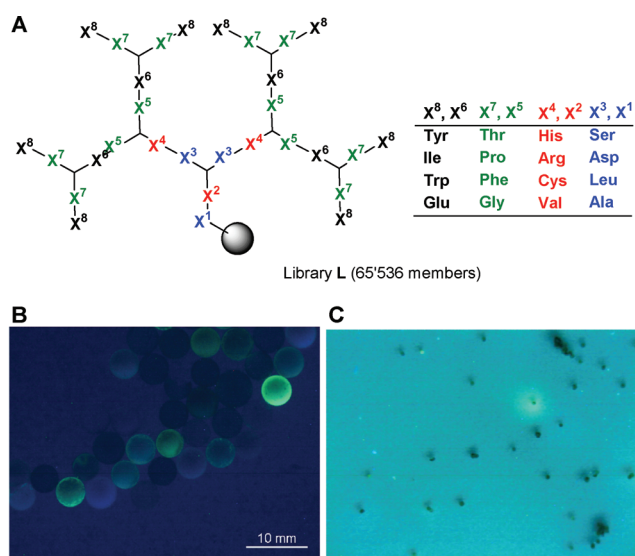


**Fig. 3** A. Combinatorial peptide dendrimer library **L**. B. On-bead screening with substrate **1b**. C. off-bead screening with substrate **1b**.

hydrophobic or aromatic residues in the outer shells of the dendrimers. Sequencing of inactive beads revealed dendrimers carrying a catalytically active core but whose activity was inhibited by anionic glutamate residues in the outer dendrimer branches, for example peptide dendrimer **D3** (AcET)<sub>8</sub>(BIG)<sub>4</sub>(BHA)<sub>2</sub>BHL (Table 1), highlighting the interplay between the outer and inner branches of the dendrimer.

One limitation of our combinatorial libraries is that the dendrimer topology is fixed and only the nature and number of the amino acids within the branches can be varied systematically.<sup>15</sup> To probe the effect of both sequence and topology on catalysis, we prepared a small 96-membered combinatorial library by SPOT synthesis.<sup>16</sup> In this method the solid support is a cellulose sheet and compounds are identified by their position on the sheet rather than by bead decoding.<sup>17</sup> The library contained linear undecapeptides and G1, G2 and G3 peptide dendrimers with up to 54 amino acids. Activity screening using substrate **1a** showed strong activity for the histidine undecapeptide **His11**. Kinetic studies of oligohistidine peptides with one to 15 residues showed that these peptides were catalytically quite active but reached a plateau of relative proficiency per histidine residue for the heptamer **His7**. Further oligomerisation did not significantly increase

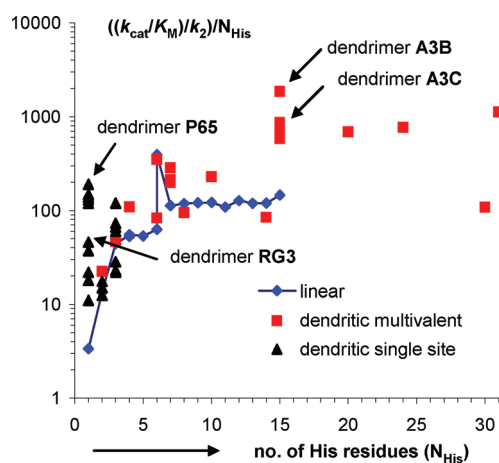


**Fig. 4** Overview of catalytic proficiencies per histidine residue for linear and dendritic histidine containing peptides, for the hydrolysis of **1a** at pH 5.5. See Table 1 for structures. Note that three histidine residues are needed per catalytic site.

catalytic proficiency per histidine up to **His15**. The peptide dendrimer **A3C** (AcHT)<sub>8</sub>(BHT)<sub>4</sub>(BHT)<sub>2</sub>BHT which also carries 15 histidines remained one order of magnitude more active than these linear peptides, highlighting that the dendritic topology was particularly well suited for catalysis (Fig. 4). By comparison, octapeptides bearing four histidine residues and reported by Schmuck *et al.* to catalyse the hydrolysis of **1a** were also much less efficient.<sup>18</sup> The SPOT library also indicated peptide dendrimer **P65** (Ac-YG)<sub>8</sub>(BYS)<sub>4</sub>(BKK)<sub>2</sub>BTH as a potent catalyst, which was confirmed by resynthesis and kinetic characterisation. Dendrimer **P65** combined catalytically productive aromatic residues in the outer branches with a catalytic core composed of four lysine residues in the G1 branch for substrate binding and a single histidine residue as catalytic group. This dendrimer showed the strongest catalytic proficiency per histidine residue for a catalyst with a single catalytic histidine residue, although partial acetylation of the lysine side chains took place during turnover. Cyclic peptides with multiple lysines and a single histidine residue designed by Vial and Dumy as ATP and heparin sensors were also highly efficient on per-histidine basis for the hydrolysis of **1b**, however in this case no lysine acylation was documented.<sup>19</sup>

A similar combinatorial strategy was used to search for aldolase peptide dendrimers in a 65 536-membered combinatorial library displaying proline as a variable amino acid at the N-termini and lysine in the G0 and G1 branches.<sup>20</sup> The target reaction was the aldolisation of 4-nitrobenzaldehyde **3** to form aldols such as **4** with cyclohexanone or the corresponding product with acetone. On-bead screening was based on staining beads carrying enamine-reactive peptide dendrimers with the tagged 1,3-diketone **5**, or by using the fluorogenic substrate dihydroxyacetone umbelliferyl ether **6** which undergoes a fluorogenic enolisation/ $\beta$ -elimination sequence in the presence of aldolase reactive catalysts (Fig. 5).<sup>21</sup> The study showed that aldolisation catalysis could be obtained with peptide dendrimers carrying multiple proline residues at their N-termini, such as dendrimer **L2D1** (PK)<sub>8</sub>(BPK)<sub>4</sub>(BYL)<sub>2</sub>BIG. Catalysis required a pair of proline residues without involvement of the lysine side chains. The positive dendritic effect observed remained quite modest (four-fold

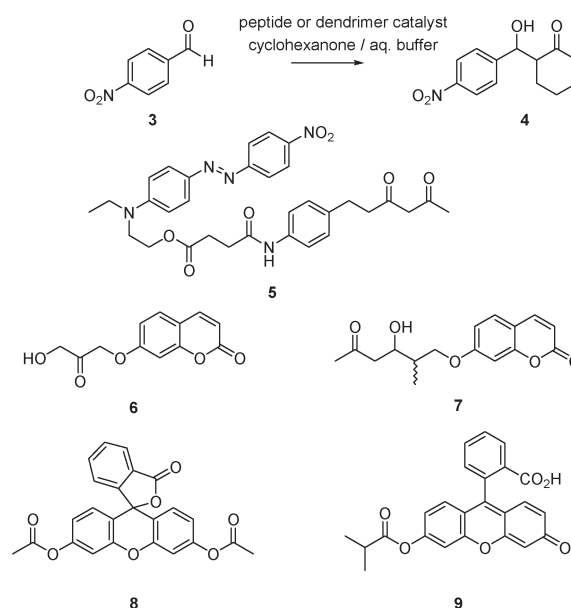


**Fig. 5** Model aldol reaction and probes used to screen combinatorial libraries for aldolase catalysis and ester hydrolysis.

higher reactivity per proline residue compared to proline alone), while enantioselectivities were either non-existent (aqueous buffer) or modest (in dimethylsulfoxide). We later identified linear aldolase octapeptides by screening a similar 65 536-membered combinatorial library using diketone **5**.<sup>22</sup> The best catalyst identified in this series, peptide **P5** (Pro-Phe-Tyr-Leu-Phe-Hyp-Val-AspNH<sub>2</sub>) was also at least 15-fold more active than proline and showed enantioselectivities that were better than in previously designed aldolase peptides.<sup>23</sup> The dendritic effect on catalysis in aldolase peptide dendrimers up to G3 was thus easily matched by optimized linear peptide catalysts. It should be noted that tripeptides with an N-terminal proline identified by Wennekers *et al.* are currently among the most enantioselective and active organocatalysts for aldol type reactions.<sup>24</sup>

We have recently investigated esterase and aldolase catalysis in a 3rd generation dendrimer combinatorial library containing only one variable amino acid per branch.<sup>25</sup> Thus, combinatorial libraries **L** (X<sup>4</sup>)<sub>8</sub>(LysX<sup>3</sup>)<sub>4</sub>(LysX<sup>2</sup>)<sub>2</sub>LysX<sup>1</sup> (X<sup>1-4</sup> = 14 different amino acids or deletion, Lys = branching lysine residue, 6750 members) and **AcL** (with N-terminal acetylation) were prepared by split-and-mix SPPS. While no activities were found with using aldolase fluorogenic substrates **6** or **7**,<sup>26</sup> histidine containing sequences were found that catalysed the hydrolysis of fluorescein diacetate **8**, a hydrophobic fluorogenic ester substrate. The dendrimers were synthesized and characterized in detail for the isobutyryl ester **9**, which shows better aqueous solubility and reproducibility in kinetic studies. Catalytically active dendrimers contained hydrophobic residues for substrate binding, such as **AcH3** (Ac-H)<sub>8</sub>(KL)<sub>4</sub>(KV)<sub>2</sub>KK. On the other hand polycationic dendrimers from library **L** with multiple free amino termini such as **H8** (H)<sub>8</sub>(K $\beta$ A)<sub>4</sub>(KT)<sub>2</sub>KaP (aP = (2S,4S)-4-aminoproline) showed stronger reactivity towards 8-acetoxypyrene-1,3,6-trisulfonate **1a**, but underwent partial acylation of N-termini during the reaction. These experiments showed the critical role played by non-catalytic amino acids in determining the substrate selectivity of peptide dendrimer esterase enzyme models.

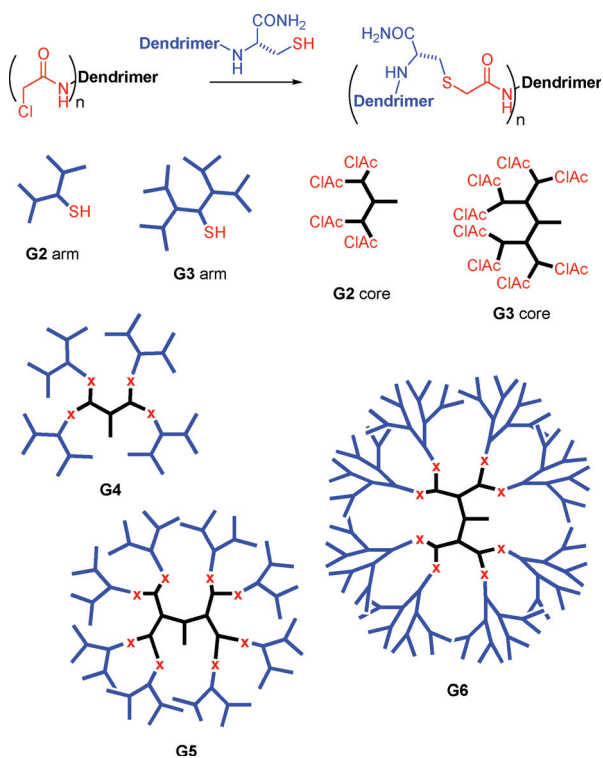


**Fig. 6** The ClAc ligation for the convergent synthesis of peptide dendrimers.

### The multivalent ClAc-ligation

The divergent synthesis of peptide dendrimers by SPPS gives good yields up to G3 peptide dendrimers with eight endgroups, but is not reliable for the synthesis of higher generation analogs, although G4 dendrimers were obtained in modest yields in selected cases.<sup>11a</sup> We have recently developed a convergent assembly strategy to access higher generation peptide dendrimers.<sup>27</sup> Convergent synthesis is the most commonly used strategy for the synthesis of dendrimers.<sup>28</sup> Our approach uses a multivalent “dendrimers-on-dendrimer” chloroacetyl cysteine (ClAc) ligation. The reaction is also known as thioether ligation,<sup>29</sup> and has been used previously only for the ligation of linear peptides to PAMAM dendrimers.<sup>30</sup> Peptide dendrimers bearing four or eight chloroacetyl groups at their N-termini are ligated with G2 and G3 peptide dendrimers with a cysteine residue at their focal point, to give G4, G5 and G6 dendrimers containing up to 341 amino acids (Fig. 6). The reaction proceeds well in slightly alkaline aqueous or aqueous/organic solvent under strict exclusion of oxygen to prevent the formation of disulfide bridged dimers of the cysteine component. The method provides a general entry into protein-sized peptide dendrimers. The ClAc ligation can be performed without protecting groups on amino acids side chains.

As an application example for the convergent synthesis of protein-sized peptide dendrimers using the multivalent ClAc ligation, we prepared higher generation analogues of the esterase and aldolase enzyme models described above. The reactions were generally high yielding and the products were readily purified by preparative HPLC to give essentially pure products.

The G4, G5 and G6 esterase dendrimers showed comparable activities to their lower generation analogues for substrate **1a**. On the other hand a strong positive dendritic effect was observed for aldolisation catalysis using dendrimers such as **G5P5**, **G6P1** (Table 1) with multiple N-terminal proline residues. In the case of the best catalyst **G6P1** the activity corresponds to a 150-fold reactivity increase per catalytic N-terminal proline compared to proline alone, for the reaction of 4-nitrobenzaldehyde with acetone in 50% aqueous acetone at pH 7.

Additional applications of the multivalent ClAc ligation in our laboratory have shown that the reaction is broadly applicable for coupling four G1, G2 or G3 peptide dendrimers on a tetrachloroacetylated G2 dendrimer core to yield G3, G4 or G5 peptide dendrimers with a variety of sequences. However the eight-fold coupling to octa-chloroacetylated G3 dendrimer cores is often more problematic. Further applications of this convergent synthesis will be reported in the near future.

### Structural studies of peptide dendrimers: random coils and $\alpha$ -helices

Peptide dendrimers give sharp peaks by <sup>1</sup>H-NMR indicative of rapid conformational equilibria on the NMR timescale, which is typical for dendrimers consisting of conformationally flexible building blocks. This is also evidenced by the observation of flattened conformations in peptide dendrimers adsorbed on surfaces by scanning tunneling microscopy (STM).<sup>31</sup> We have investigated in detail the structure of the single site esterase peptide dendrimer **RG3** described above. Its hydrodynamic radius of  $R_h = 1.44$  nm can be determined by using diffusion NMR, which in terms of compactness corresponds to a molten globule state. Circular dichroism (CD) showed that **RG3** does not contain significant secondary structures. A molecular dynamics (MD) study was performed on dendrimer **RG3** and its analog **HG3**,<sup>32</sup> which confirmed the molten globule state of the dendrimer and the random coil nature of its peptide backbone. On average only one in ten backbone peptide bonds was participating in a backbone-to-backbone hydrogen bond, in sharp contrast to folded secondary structures in which all peptide bonds are hydrogen bonded to other backbone amides. Similar data were reported in an extended MD simulation of dendrimer **B1**.<sup>33</sup>

A docking study was performed to understand the interactions between the fluorogenic ester substrate **1b** and the dendrimers.<sup>32</sup> The docking study showed that for the case of dendrimer **RG3** the pyrene group of substrate **1b** interacted strongly with the aromatic residues in the G2 and G3 dendrimer branches. In the case of dendrimer **HG3** which contained only hydrophobic amino acids in the G2 and G3 dendrimer branches no binding interaction took place in docking between substrate **1b** and these outer branches. This docking study was consistent with the observation of a positive effect on catalysis upon addition of the outer dendrimer branches in dendrimer **RG3**, but no effect in dendrimer **HG3** (Fig. 7a). The effect was confirmed in the analog **RG3H** (AcYT)<sub>8</sub>(BWG)<sub>4</sub>(BHS)<sub>2</sub>BHS incorporating the G2 and G3 branches of **RG3** and the more active catalytic core of **HG3**. This dendrimer showed a 10-fold higher rate acceleration  $k_{cat}/k_{uncat}$  for the hydrolysis of **1b** compared to **HG3** and **RG3**.<sup>34</sup>

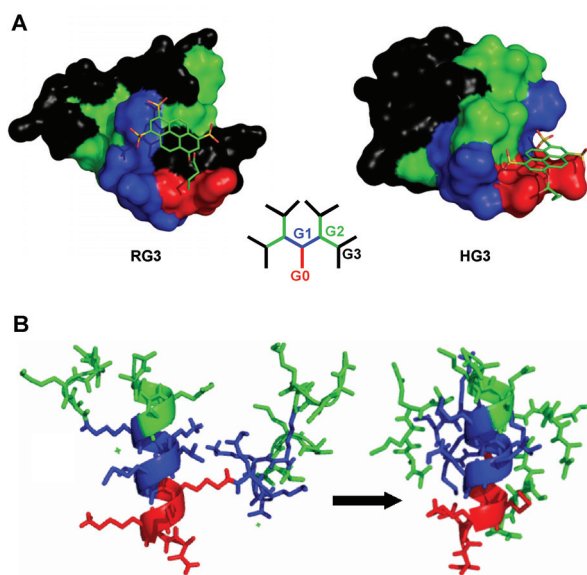


**Fig. 7** A. Docking model of dendrimers **RG3** and **HG3** with bound substrate **1b**. B. MD simulation of the folding of  $\alpha$ -helical peptide dendrimer  **$\alpha$ D3**.

The absence of stable secondary structures in peptide dendrimer **RG3** and related dendrimers with short dipeptide branches prompted us to test if secondary structures would be observable at all within a peptide dendrimer with short branches. To this end we prepared a series of G1 and G2 peptide dendrimers with heptapeptide respectively tetrapeptide branches containing typical  $\alpha$ -helical sequences. This experiment led to the identification of dendrimer  **$\alpha$ D3** (AcAMEA)<sub>4</sub>(KKLME)<sub>2</sub>KMKLA which exhibits 57%  $\alpha$ -helix content at 25 °C, pH 3.8 with 20% trifluoroethanol, as measured by CD and FT-IR.<sup>35</sup> This is comparable to the secondary structure content of the control linear peptide **L3** with alanine replacing the branching lysine residues (49%  $\alpha$ -helix under the same conditions). In this case MD showed that while the  $\alpha$ -helix is partly unfolded in the linear peptide **L3**, the  $\alpha$ -helix is fully stable within peptide dendrimer  **$\alpha$ D3** along its  $\alpha$ -peptide branch, while the other dendrimer branches grown from the  $\epsilon$ -lysine amino groups are wrapped around it (Fig. 7b).

#### Metallo-peptide dendrimers: cobalamin ligands and bipyridine containing peptide dendrimers

In our efforts to explore the chemistry of metal binding peptide dendrimers, we have investigated peptide dendrimer **B1** (AcES)<sub>8</sub>(BEA)<sub>4</sub>(KAmbY)<sub>2</sub>BCD, which has a cysteine at its core and forms a stable complex with cobalamin (vitamin B<sub>12</sub>). Binding to cobalamin involves coordination of the cysteine thiol side chain at cobalt and represents a simple model for cobalamin transport proteins.<sup>36</sup> Dendrimer **B1** was obtained by on-bead colorimetric screening of a combinatorial library for binding to cobalamin, followed by iterative structure optimization. The outer branches of **B1** carry twelve glutamate residues, a characteristic feature occurring in the majority of dendrimers identified in the combinatorial vitamin B<sub>12</sub> binding experiments. Glutamate

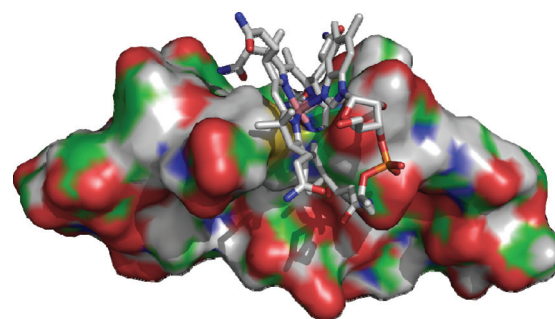


**Fig. 8** Model of the **B1**-cobalamin complex from MD.

residues were also a constant feature in B<sub>12</sub> binding cyclic peptides identified in a similar combinatorial screening.<sup>37</sup>

A critical role of charged residues in cobalamin-peptide dendrimer binding kinetics was suggested by the very slow binding of cobalamin with cationic analogue **B1K** (AcKS)<sub>8</sub>(BKA)<sub>4</sub>(KAmbY)<sub>2</sub>BCL bearing lysines in place of the glutamates. These observations prompted us to investigate the role of the glutamate residues in the vitamin B<sub>12</sub>-dendrimer interaction. A systematic investigation of the effect of substituting neutral glutamines for anionic glutamates showed that the glutamates enhance the rate of binding to vitamin B<sub>12</sub>, but at the same time destabilise the corresponding complex. The polyanionic dendrimer **B1** thus showed the fastest rate of binding, but its glutamine analog **N3** (AcQS)<sub>8</sub>(BQA)<sub>4</sub>(BAmbY)<sub>2</sub>BCD with twelve glutamine residues formed a more stable complex.<sup>38</sup>

Both the free and B<sub>12</sub>-coordinated dendrimers were found to exist as random coil structures as shown by FTIR investigations. Complex formation led to more compact structures as evidenced by determination of hydrodynamic radii by diffusion NMR. The more compact structure of the complexes indicated a hydrophobic collapse of the dendrimer upon cobalamin binding. The glutamine containing dendrimer **N3** and its cobalamin complex were both more compact compared to **B1** and its complex, which might explain the stronger binding to B<sub>12</sub> by the formation of tighter contacts. A molecular dynamics study of complex formation with **B1** confirmed the hypothesis of hydrophobic collapse (Fig. 8).<sup>38</sup>

In a related study we found that the electrostatic charges in the outer branches of peptide dendrimers could also control the coordination of Fe(II) to a bipyridyl amino acid (Bpy) at the core.<sup>39</sup> Thus while bipyridyl dendrimer **E1** (AcET)<sub>4</sub>(BEV)<sub>2</sub>-BBpy $\beta$ AD identified by combinatorial screening and bearing 7 anionic carboxylates bound strongly with Fe(II) as expected for bipyridyl-type ligands, metal binding was completely inhibited in the cationic analog **E3** (AcRK)<sub>4</sub>(BFK)<sub>2</sub>BBpy $\beta$ AY with 10 positive charges in the outer dendrimer branches.

#### Bioactive peptide dendrimers

##### Glycopeptide dendrimers for drug delivery

One of the frequently envisioned applications for dendrimers is targeted drug delivery of cytotoxic drugs in cancer therapy, with the aim of increasing the therapeutic ratio by avoiding unwanted toxicity in non-target tissues,<sup>40</sup> in particular using relatively large dendrimers with multiple copies of a drug,<sup>41</sup> capitalizing

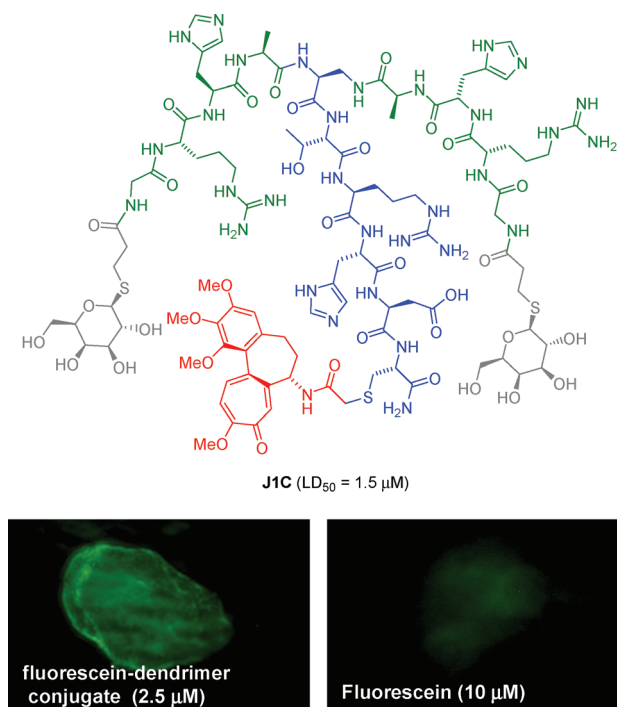


**Fig. 9** Structure of **J1C** and binding of its fluorescein conjugate to Jurkat cells.

on the enhanced permeation and retention effect.<sup>42</sup> We have investigated the use of our peptide dendrimers for drug targeting at the example of glycopeptide dendrimer colchicine conjugates. Our strategy aims at obtaining a cell-targeting, non-toxic precursor which would liberate the active drug upon proteolysis inside the cell. Colchicine is a cytotoxic microtubule destabilising natural product. Early experiments aimed at targeting cancer cells *via* galectins showed that various glycopeptide dendrimer conjugates of colchicine such and conjugate **20** (Glc-β-ON=Ac)<sub>8</sub>(BL)<sub>4</sub>(BD)<sub>2</sub>BC(SCol)H were cytotoxic to cancer cells. The mechanism of action of this conjugate involved disruption of the cytoskeleton as observed with colchicine.<sup>43</sup>

A follow-up experiment based on direct screening of a combinatorial library of galactosylated G1 peptide dendrimers for binding to cancer cells in culture allowed to identify further examples of cytotoxic colchicine conjugates such as **J1C** (GalB-GRHA)<sub>2</sub>BTRHDC(Col) (Fig. 9).<sup>44</sup> Selective binding of the galactosylated peptide dendrimers to cancer cells was demonstrated by fluorescence activated cell sorting (FACS) and confocal microscopy using fluorescein conjugates such as **J1F** (GalB-GRHA)<sub>2</sub>BTRHDC(Fluo). The role of galactose was evidenced by the fact that the corresponding non-galactosylated dendrimers were inactive. However, the bioactivity of the conjugates remained modest (IC<sub>50</sub> = 1.5 μM), probably due to the weak tubulin binding activity of the dendrimer-colchicine conjugate and its proteolysed fragments within the cells.

#### Glycopeptide dendrimers as *Pseudomonas aeruginosa* biofilm inhibitors

The peptide dendrimer architecture has proven well suited for the multivalent display of glycosyl groups to bind lectins, a class

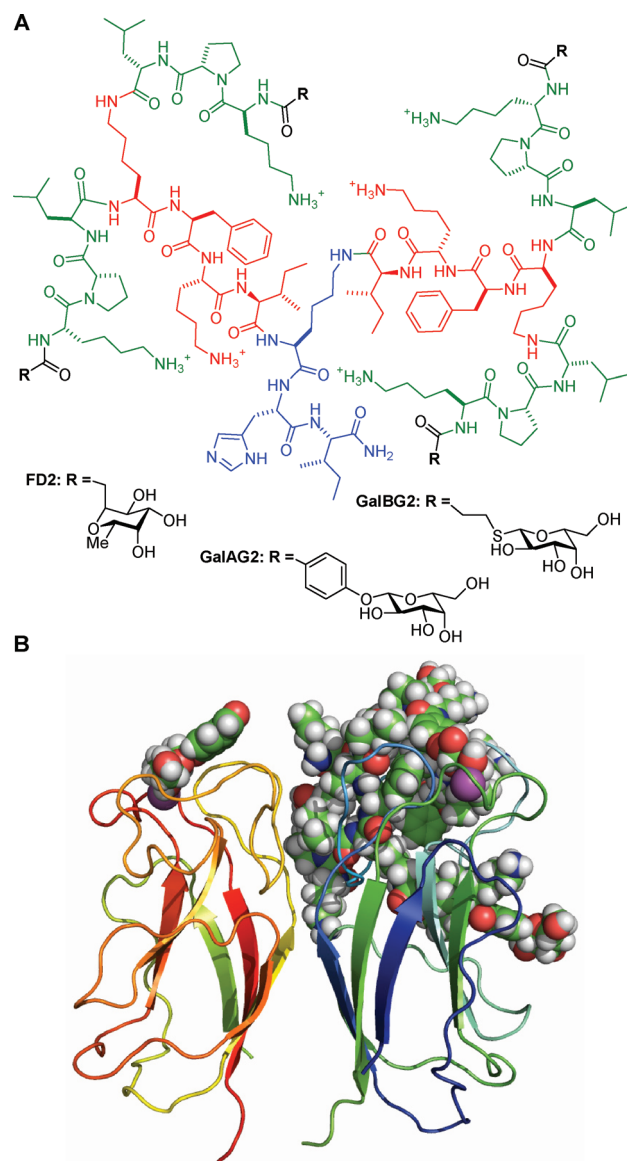


**Fig. 10** **A.** Structure of glycopeptide dendrimer biofilm inhibitors. **B.** Model of a 1 : 1 complex of dendrimer **GalAG2** (in cpk) with **LecA** (ribbons).

of carbohydrate binding proteins known to be sensitive to multivalent interactions.<sup>45</sup> We have focused on targeting the microbial lectins **LecA** (PA-IL)<sup>46</sup> and **LecB** (PA-III),<sup>47</sup> which mediate biofilm formation in the opportunistic pathogen *Pseudomonas aeruginosa*. This bacterium exhibits multi-antibiotic resistance and is a primary cause of death in cystic fibrosis.<sup>48</sup> Biofilm inhibition offers a promising alternative therapeutic strategy. Screening a combinatorial library of fucosylated peptide dendrimers led to the glycopeptide dendrimer **FD2** as a potent **LecB** ligand (Fig. 10a).<sup>49,15</sup> This dendrimer binds the lectin with submicromolar IC<sub>50</sub>, and shows potent inhibition of *P. aeruginosa* biofilms for both the laboratory strain PAO1 and for several antibiotic resistant clinical isolates.<sup>50</sup> A structure-activity relationship study with lower and higher generation analogs such as **2G3** (cFuc-KP)<sub>8</sub>(KLF)<sub>4</sub>(KKI)<sub>2</sub>KHI (IC<sub>50</sub> = 25 nM for binding to **LecB**),<sup>51</sup> as well as the diastereoisomeric analog incorporating D-amino acids **D-FD2** (cFuc-kpl)<sub>4</sub>(Kfkl)<sub>2</sub>Khl,<sup>52</sup> showed that

lectin binding depended on multivalency as well as on the amino acid sequence and length of the dendrimer branches. X-ray structure determination of the c-fucosylated tripeptide G2-branch of **FD2** in complex with LecB allowed to build a model of the peptide dendrimer lectin complex.<sup>50</sup>

Appending the peptide dendrimer portion of **FD2** with  $\beta$ -galactosyl endgroups gave dendrimers **GalAG2** (GalA-KPL)<sub>4</sub> (KFKI)<sub>2</sub>KHI and **GalBG2** (GalB-KPL)<sub>4</sub>(KFKI)<sub>2</sub>KHI as potent ligands for the galactose specific lectin LecA, which also acted as biofilm inhibitors (Fig. 10).<sup>53</sup> Structure–activity relationship studies showed that multivalency was essential for lectin binding and for biofilm inhibition. In this case a crystallographic study showed that the aromatic aglycone group of the galactosyl ligand in **GalAG2** engaged in a key T-stack interaction with a histidine residue near the galactose binding site of LecA, enabling further contacts with the G2-tripeptide arm. By contrast structure determination of the galactosylated G2 tripeptide of **GalBG2** in complex with LecA showed that its tripeptide was disordered, explaining the lower binding affinity of this ligand. Several other glycodendrimers constructs have been reported as ligands for LecA and LecB,<sup>54</sup> however their possible effect as biofilm inhibitor has thus far not been documented. In a related approach, we have found that peptide dendrimers with multivalent display of  $\alpha$ -mannosyl groups next to aromatic residues are potent ligands to concanavalin A, showing the generality of the peptide dendrimer approach to multivalent lectin ligands.<sup>55</sup>

### Membrane disrupting antimicrobial peptide dendrimers with multiple amino termini

Many antimicrobial peptides (AMP) act by disrupting microbial membranes, an effect which is observed for molecules containing multiple positive charges together with hydrophobic groups, whereby an amphiphilic architecture is believed to be crucial.<sup>56</sup> In AMPs the multiple positive charges necessary for membrane disruption are brought about by the side chains of basic amino acids. Using a bead diffusion assay for screening antimicrobial activity in combinatorial libraries,<sup>57</sup> we have recently discovered antimicrobial peptide dendrimers such as **H1** L<sub>8</sub>(KL)<sub>4</sub>(KF)<sub>2</sub>KK and **bH1** L<sub>8</sub>(BL)<sub>4</sub>(BF)<sub>2</sub>BK (MIC = 2–4  $\mu\text{g mL}^{-1}$  against *B. subtilis* and *E. Coli*) in which positive charges are provided by the multiple amino termini at the dendrimer periphery rather than by amino acid side chains (Fig. 11).<sup>58</sup> These dendrimers act as membrane disrupting agents and show remarkably low hemolytic activity. Optimization of their activity against specific strains is currently ongoing and represents a new opportunity to develop non-toxic antimicrobial agents.

### Proteolysis of peptide dendrimers

The ability of proteins and peptides to undergo proteolysis is essential to their biological function since it represents an obligatory pathway for metabolism and deactivation. Using trypsin and  $\alpha$ -chymotrypsin cleavage sites as models, we have found that the protease reactivity of peptide dendrimers can be controlled by the degree of branching.<sup>59</sup> Dendrimers with two or three amino acids between branching points are readily cleaved by trypsin irrespective of the position of the reactive peptide

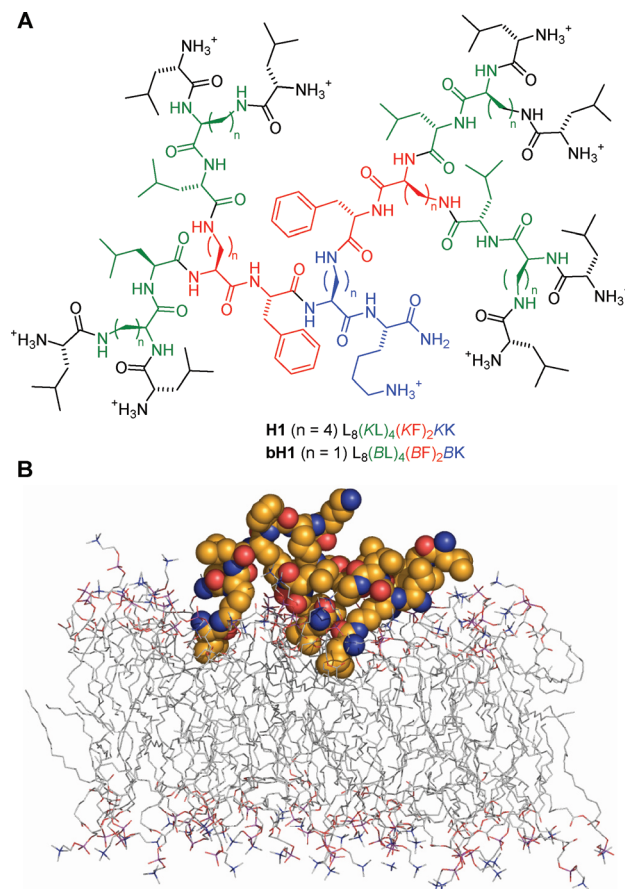


**Fig. 11** A. Antimicrobial peptide dendrimers. B. MD simulation of dendrimer **H1** interacting with a phosphatidyl choline membrane.

bond. For example dendrimer **D12** (Ac-Ser-Ala)<sub>8</sub>(Dap-Ala-Arg<sup>1</sup>)<sub>4</sub>(Dap-Ala-Asp)<sub>2</sub>Dap-Phe-Ala-Lys(Fluo)NH<sub>2</sub> (1 = cleavage site) is cleaved by trypsin as fast as its linear peptide analog (Ala instead of Dap). On the other hand proteolysis is blocked in more compact dendrimers with only one amino acid per branch, such as **D18B** (Ac-Glu)<sub>8</sub>(Dap-Phe)<sub>4</sub>(Dap-Arg)<sub>2</sub>Dap-LeuNH<sub>2</sub>.

This study provides general guidelines to design protease reactive versus protease resistant peptide dendrimers. Proteolysis in a peptide dendrimer can also be controlled by using non-natural amino acids such as  $\beta$ -amino acids or D-amino acids, although their use should be taken with caution since they might induce unwanted toxicity. The control of proteolysis by topology provides a unique possibility to tune the degradation behaviour of peptide dendrimers, in particular for drug delivery applications.

### Conclusion and outlook

The use of branching diamino acids during SPPS provides rapid access to a variety of peptide and glycopeptide dendrimers equipped with amino acid side chains throughout the structure in an “apple tree” configuration. These side chains can be used for providing specific functional groups (e.g. catalysis) or be chosen for fine-tuning the physicochemical properties of the dendrimers. Screening of combinatorial libraries and optimisation by amino acid sequence variations leads to dendrimers with catalysis and ligand binding properties.



Peptide dendrimers with an “apple tree” configuration combine properties of organic dendrimers such as multivalency and dendritic effect resulting from proximity effects with properties typical for peptides and proteins such as enzyme-like catalysis and susceptibility to degradation by proteases. In addition unique properties are also observed such as solubility in aqueous media without formation of aggregates and suppression of proteolysis by modulating the dendrimer structure. The screening of combinatorial libraries with an easy decoding procedure derived from the branching structures allows the discovery of peptide dendrimers with new structures and properties. Future developments include the synthesis and testing of larger peptide dendrimers with molecular weight approaching small proteins and more detailed physicochemical studies of active dendrimers. We believe that many more functional peptide and glycopeptide dendrimers remain to be discovered and optimized by chemical synthesis and testing as described in this review

## Acknowledgements

This work was supported financially by the University of Berne, the Swiss National Science Foundation, and the European Union FP7-ITN-238434.

## Notes and references

- J. L. Reymond, R. Van Deursen, L. C. Blum and L. Ruddigkeit, *Med. Chem. Commun.*, 2010, **1**, 30–38.
- (a) G. R. Newkome, C. N. Moorefield and F. Vögtle, *Dendritic Molecules: Concepts, Synthesis, Applications*, VCH, Weinheim, 2001; (b) C. C. Lee, J. A. MacKay, J. M. J. Fréchet and F. C. Szoka, *Nat. Biotechnol.*, 2005, **23**, 1517–1526; (c) D. Astruc, E. Boisselier and C. Ornelas, *Chem. Rev.*, 2010, **110**, 1857–1959.
- J. Kofoed and J. L. Reymond, *Curr. Opin. Chem. Biol.*, 2005, **9**, 656–664.
- (a) K. Sadler and J. P. Tam, *J. Biotechnol.*, 2002, **90**, 195–229; (b) L. Crespo, G. Sanclimens, M. Pons, E. Giralt, M. Royo and F. Albericio, *Chem. Rev.*, 2005, **105**, 1663–1681; (c) P. Niederhafner, J. Sebestien and J. Jezek, *J. Pept. Sci.*, 2005, **11**, 757–788.
- (a) A. Esposito, E. Delort, D. Lagnoux, F. Djojo and J. L. Reymond, *Angew. Chem., Int. Ed.*, 2003, **42**, 1381–1383; (b) T. Darbre and J. L. Reymond, *Acc. Chem. Res.*, 2006, **39**, 925–934; (c) T. Darbre and J. L. Reymond, *Curr. Top. Med. Chem.*, 2008, **8**, 1286–1293.
- B. Merrifield, *Methods Enzymol.*, 1997, **289**, 3–13.
- (a) A. Clouet, T. Darbre and J. L. Reymond, *Adv. Synth. Catal.*, 2004, **346**, 1195–1204; (b) C. Douat-Casassus, T. Darbre and J. L. Reymond, *J. Am. Chem. Soc.*, 2004, **126**, 7817–7826; (c) D. Lagnoux, E. Delort, C. Douat-Casassus, A. Esposito and J. L. Reymond, *Chem.–Eur. J.*, 2004, **10**, 1215–1226.
- (a) R. Breslow, *Acc. Chem. Res.*, 1995, **28**, 146–153; (b) L. Baltzer, H. Nilsson and J. Nilsson, *Chem. Rev.*, 2001, **101**, 3153–3163; (c) A. J. Kirby and F. Hollfelder, *From Enzyme Models to Model Enzymes*, 2009, Royal Society of Chemistry, Cambridge, UK.
- (a) A. Clouet, T. Darbre and J. L. Reymond, *Angew. Chem., Int. Ed.*, 2004, **43**, 4612–4615; (b) A. Clouet, T. Darbre and J. L. Reymond, *Biopolymers*, 2006, **84**, 114–123; (c) N. Maillard, A. Clouet, T. Darbre and J. L. Reymond, *Nat. Protoc.*, 2009, **4**, 132–142.
- J. L. Reymond, V. S. Fluxa and N. Maillard, *Chem. Commun.*, 2009, 34–46.
- (a) E. Delort, T. Darbre and J. L. Reymond, *J. Am. Chem. Soc.*, 2004, **126**, 15642–15643; (b) E. Delort, N. Q. Nguyen-Trung, T. Darbre and J. L. Reymond, *J. Org. Chem.*, 2006, **71**, 4468–4480.
- (a) K. S. Lam, M. Lebl and V. Krchnak, *Chem. Rev.*, 1997, **97**, 411–448; (b) K. S. Lam, S. E. Salmon, E. M. Hersh, V. J. Hruby, W. M. Kazmierski and R. J. Knapp, *Nature*, 1991, **354**, 82–84; (c) R. A. Houghten, C. Pinilla, S. E. Blondelle, J. R. Appel, C. T. Dooley and J. H. Cuervo, *Nature*, 1991, **354**, 84–86; (d) A. Furka, F. Sebestyén, M. Asgedom and G. Dibo, *Int. J. Pept. Protein Res.*, 1991, **37**, 487–493.
- N. Maillard, T. Darbre and J. L. Reymond, *J. Comb. Chem.*, 2009, **11**, 667–675.
- S. Javor, E. Delort, T. Darbre and J. L. Reymond, *J. Am. Chem. Soc.*, 2007, **129**, 13238–13246.
- E. M. V. Johansson, E. Kolomiets, F. Rosenau, K.-E. Jaeger, T. Darbre and J.-L. Reymond, *New J. Chem.*, 2007, **31**, 1291–1299.
- R. Biswas, N. Maillard, J. Kofoed and J. L. Reymond, *Chem. Commun.*, 2010, **46**, 8746–8748.
- R. Frank, *J. Immunol. Methods*, 2002, **267**, 13–26.
- C. Schmuck, U. Michels and J. Dudaczek, *Org. Biomol. Chem.*, 2009, **7**, 4362–4368.
- (a) L. Vial and P. Dumy, *J. Am. Chem. Soc.*, 2007, **129**, 4884–4885; (b) L. Vial and P. Dumy, *ChemBioChem*, 2008, **9**, 2950–2953.
- J. Kofoed, T. Darbre and J. L. Reymond, *Org. Biomol. Chem.*, 2006, **4**, 3268–3281.
- (a) J. Kofoed, T. Darbre and J. L. Reymond, *Chem. Commun.*, 2006, 1482–1484; (b) R. Sicart, M. P. Collin and J. L. Reymond, *Biotechnol. J.*, 2007, **2**, 221–231.
- J. Kofoed and J. L. Reymond, *J. Comb. Chem.*, 2007, **9**, 1046–1052.
- J. Kofoed, J. Nielsen and J. L. Reymond, *Bioorg. Med. Chem. Lett.*, 2003, **13**, 2445–2447.
- (a) J. D. Revell and H. Wennemers, *Curr. Opin. Chem. Biol.*, 2007, **11**, 269–278; (b) M. Wiesner, G. Uper, G. Angelici and H. Wennemers, *J. Am. Chem. Soc.*, 2010, **132**, 6–7.
- N. Maillard, R. Biswas, T. Darbre and J. L. Reymond, *ACS Comb. Sci.*, 2011, **13**, 310–230.
- R. Perez Carlon, N. Jourdain and J. L. Reymond, *Chem.–Eur. J.*, 2000, **6**, 4154–4162.
- N. A. Uhlich, T. Darbre and J. L. Reymond, *Org. Biomol. Chem.*, 2011, **9**, 7071–7084.
- (a) S. M. Grayson and J. M. J. Fréchet, *Chem. Rev.*, 2001, **101**, 3819–3867; (b) G. R. Newkome and C. Shreiner, *Chem. Rev.*, 2010, **110**, 6338–6442.
- (a) W. Lindner and F. A. Robey, *Int. J. Pept. Protein Res.*, 1987, **30**, 794–800; (b) P. E. Dawson and S. B. H. Kent, *J. Am. Chem. Soc.*, 1993, **115**, 7263–7266; (c) J. O. Freeman, W. C. Lee, M. E. P. Murphy and J. C. Sherman, *J. Am. Chem. Soc.*, 2009, **131**, 7421–7429.
- M. Sakamoto, A. Ueno and H. Mihara, *Chem. Commun.*, 2000, 1741–1742.
- E. Delort, E. Szocs, R. Widmer, H. Siegenthaler and J. L. Reymond, *Macromol. Biosci.*, 2007, **7**, 1024–1031.
- S. Javor and J. L. Reymond, *J. Org. Chem.*, 2009, **74**, 3665–3674.
- L. C. Filipe, M. Machuqueiro and A. M. Baptista, *J. Am. Chem. Soc.*, 2011, **133**, 5042–5052.
- S. Javor and J.-L. Reymond, *Isr. J. Chem.*, 2009, **49**, 129–136.
- S. Javor, A. Natalello, S. M. Doglia and J. L. Reymond, *J. Am. Chem. Soc.*, 2008, **130**, 17248–17249.
- P. Sommer, N. A. Uhlich, J. L. Reymond and T. Darbre, *ChemBioChem*, 2008, **9**, 689–693.
- V. Dulery, N. A. Uhlich, N. Maillard, V. S. Fluxa, J. Garcia, P. Dumy, O. Renaudet, J. L. Reymond and T. Darbre, *Org. Biomol. Chem.*, 2008, **6**, 4134–4141.
- N. A. Uhlich, A. Natalello, R. U. Kadam, S. M. Doglia, J. L. Reymond and T. Darbre, *ChemBioChem*, 2010, **11**, 358–365.
- N. A. Uhlich, P. Sommer, C. Buhr, S. Schurch, J. L. Reymond and T. Darbre, *Chem. Commun.*, 2009, 6237–6239.
- A. K. Patri, J. F. Kukowska-Latallo and J. R. Baker Jr, *Adv. Drug Delivery Rev.*, 2005, **57**, 2203–2214.
- M. E. Fox, F. C. Szoka and J. M. J. Fréchet, *Acc. Chem. Res.*, 2009, **42**, 1141–1151.
- R. Duncan, *Nat. Rev. Cancer*, 2006, **6**, 688–701.
- D. Lagnoux, T. Darbre, M. L. Schmitz and J. L. Reymond, *Chem.–Eur. J.*, 2005, **11**, 3941–3950.
- E. M. Johansson, J. Dubois, T. Darbre and J. L. Reymond, *Bioorg. Med. Chem.*, 2010, **18**, 6589–6597.
- (a) Y. C. Lee and R. T. Lee, *Acc. Chem. Res.*, 1995, **28**, 321–327; (b) J. J. Lundquist and E. J. Toone, *Chem. Rev.*, 2002, **102**, 555–578.
- E. Mitchell, C. Houles, D. Sudakevitz, M. Wimmerova, C. Gautier, S. Perez, A. M. Wu, N. Gilboa-Garber and A. Imberty, *Nat. Struct. Biol.*, 2002, **9**, 918–921.
- (a) R. Loris, D. Tielker, K. E. Jaeger and L. Wyns, *J. Mol. Biol.*, 2003, **331**, 861–870; (b) A. Imberty, M. Wimmerova, E. P. Mitchell and N. Gilboa-Garber, *Microbes Infect.*, 2004, **6**, 221–228.

- 48 V. E. Wagner and B. H. Iglewski, *Clin. Rev. Allergy Immunol.*, 2008, **35**, 124–134.
- 49 E. Kolomiets, E. M. Johansson, O. Renaudet, T. Darbre and J. L. Reymond, *Org. Lett.*, 2007, **9**, 1465–1468.
- 50 E. M. Johansson, S. A. Crusz, E. Kolomiets, L. Buts, R. U. Kadam, M. Cacciarini, K. M. Bartels, S. P. Diggle, M. Camara, P. Williams, R. Loris, C. Nativi, F. Rosenau, K. E. Jaeger, T. Darbre and J. L. Reymond, *Chem. Biol.*, 2008, **15**, 1249–1257.
- 51 E. Kolomiets, M. A. Swiderska, R. U. Kadam, E. M. Johansson, K. E. Jaeger, T. Darbre and J. L. Reymond, *ChemMedChem*, 2009, **4**, 562–569.
- 52 E. M. V. Johansson, R. U. Kadam, G. Rispoli, S. A. Crusz, K.-M. Bartels, S. P. Diggle, M. Camara, P. Williams, K.-E. Jaeger, T. Darbre and J.-L. Reymond, *Med. Chem. Commun.*, 2011, **2**, 418–420.
- 53 R. U. Kadam, M. Bergmann, M. Hurley, D. Garg, M. Cacciarini, M. A. Swiderska, C. Nativi, M. Sattler, A. R. Smyth, P. Williams, M. Camara, A. Stocker, T. Darbre and J. L. Reymond, *Angew. Chem., Int. Ed.*, 2011, **50**, 10631–10635.
- 54 (a) K. Marotte, C. Prévile, C. Sabin, M. Moumé-Pymbock, A. Imberty and R. Roy, *Org. Biomol. Chem.*, 2007, **5**, 2953–2961; (b) Y. M. Chabre, D. Giguère, B. Blanchard, J. Rodrigue, S. Rocheleau, M. Neault, S. Rauthu, A. Papadopoulos, A. A. Arnold, A. Imberty and R. Roy, *Chem.–Eur. J.*, 2011, **17**, 6545–6562.
- 55 (a) R. Euzen and J. L. Reymond, *Mol. BioSyst.*, 2011, **7**, 411–421; (b) R. Euzen and J. L. Reymond, *Bioorg. Med. Chem.*, 2011, **19**, 2879–2887.
- 56 (a) M. N. Melo, R. Ferre and M. A. Castanho, *Nat. Rev. Microbiol.*, 2009, **7**, 245–250; (b) S. P. Liu, L. Zhou, R. Lakshminarayanan and R. W. Beuerman, *Int. J. Pept. Res. Ther.*, 2011, **16**, 199–213.
- 57 V. S. Fluxa, N. Maillard, M. G. Page and J. L. Reymond, *Chem. Commun.*, 2011, **47**, 1434–1436.
- 58 M. Stach, N. Maillard, R. U. Kadam, D. Kalbermatter, M. Meury, M. G. P. Page, D. Fotiadis, T. Darbre and J. L. Reymond, *Med. Chem. Commun.*, 2012, **3**, 86–89.
- 59 P. Sommer, V. S. Fluxa, T. Darbre and J. L. Reymond, *ChemBioChem*, 2009, **10**, 1527–1536.